The American Journal of Pathology, Vol. 181, No. 6, December 2012

http://dx.doi.org/10.1016/j.ajpath.2012.08.017

Gastrointestinal, Hepatobiliary, and Pancreatic Pathology

Transgenic Expression of Interferon-γ in Mouse Stomach Leads to Inflammation, Metaplasia, and Dysplasia

Li-Jyun Syu,* Mohamad El-Zaatari,† Kathryn A. Eaton,‡§ Zhiping Liu,¶ Manas Tetarbe,* Theresa M. Keeley,¶ Joanna Pero,* Jennifer Ferris,* Dawn Wilbert,* Ashley Kaatz,* Xinlei Zheng,* Xiotan Qiao,‖ Marina Grachtchouk,* Deborah L. Gumucio,‖ Juanita L. Merchant,†¶ Linda C. Samuelson,†¶ and Andrzej A. Dlugosz*‖

From the Departments of Dermatology, Internal Medicine,† Microbiology and Immunology,§ Molecular and Integrative Physiology,¶ and Cell and Developmental Biology,‖ and the Unit for Laboratory Animal Medicine,‡ School of Medicine, University of Michigan, Ann Arbor, Michigan*

Gastric adenocarcinoma is one of the leading causes of cancer mortality worldwide. It arises through a stepwise process that includes prominent inflammation with expression of interferon-γ (IFN-γ) and multiple other pro-inflammatory cytokines. We engineered mice expressing IFN-γ under the control of the stomach-specific H^+/K^+ ATPase β promoter to test the potential role of this cytokine in gastric tumorigenesis. Stomachs of *H/K-IFN-γ* transgenic mice exhibited inflammation, expansion of myofibroblasts, loss of parietal and chief cells, spasmolytic polypeptide expressing metaplasia, and dysplasia. Proliferation was elevated in undifferentiated and metaplastic epithelial cells in *H/K-IFN-γ* transgenic mice, and there was increased apoptosis. *H/K-IFN-γ* mice had elevated levels of mRNA for IFN-γ target genes and the pro-inflammatory cytokines IL-6, IL-1β, and tumor necrosis factor-α. Intracellular mediators of IFN-γ and IL-6 signaling, pSTAT1 and pSTAT3, respectively, were detected in multiple cell types within stomach. *H/K-IFN-γ* mice developed dysplasia as early as 3 months of age, and 4 of 39 mice over 1 year of age developed antral polyps or tumors, including one adenoma and one adenocarcinoma, which expressed high levels of nuclear β-catenin. Our data identified IFN-γ as a pivotal secreted factor that orchestrates complex changes in inflammatory, epithelial, and mesenchymal cell populations to drive preneoplastic progression in stomach; however, additional alterations appear to be required for malignant conversion. *(Am J Pathol 2012, 181:2114–2125; http://dx.doi.org/10.1016/j.ajpath.2012.08.017)*

Gastric adenocarcinoma is one of the most common causes of cancer-related deaths worldwide,[1] and although the incidence of these cancers in the United States is decreasing, the 5-year survival rate is a dismal 27%.[2] Gastric cancer in humans develops through a series of stages, first defined by Correa and Piazuelo, which includes gastritis, atrophy, intestinal metaplasia, dysplasia, and carcinoma.[3] Infection with *Helicobacter pylori* is the greatest single risk factor for the development of gastric cancer.[4] The gastritis that accompanies *Helicobacter* infection plays a major role in gastric cancer development[5]; however, the key inflammatory mediators driving this process have not been fully defined. Data from several types of malignancy point to critical functions for inflammation in cancer,[6] with an interplay between extrinsic factors (infection/inflammation) and intrinsic factors (oncogenes/tumor suppressor genes) driving neoplastic progression.[7] Targeting pivotal pro-tumorigenic cytokines may thus be useful for the treatment or prevention of certain types of cancer.[8]

Interaction of *Helicobacter* with epithelial cells in the gastric corpus triggers an immune response that leads to the production of multiple cytokines and the establishment of chronic inflammation. Polymorphisms in the *IL-1β* gene predispose to gastric cancer development in humans,[9,10] and overexpression of IL1β in the corpus of transgenic mice leads to gastric dysplasia and cancer,[11] pointing to an important role for this cytokine in gastric

Supported by NIH grants DK062041 (A.A.D., D.L.G., J.L.M.) and CA118875 (A.A.D.).

Accepted for publication August 30, 2012.

Supplemental material for this article can be found at *http://ajp.amjapathol.org* or at *http://dx.doi.org/10.1016/j.ajpath.2012.08.017*.

Address reprint requests to Andrzej A. Dlugosz, M.D., University of Michigan Medical School, 3316 CC, SPC 5932, 1500 East Medical Center Drive, Ann Arbor, MI 48109. E-mail: dlugosza@umich.edu.

tumorigenesis. A Th1-polarized immune response, characterized by elevated expression of interferon-γ (IFN-γ), is activated in *Helicobacter*-infected stomach and appears to be required for preneoplastic changes, including parietal cell atrophy and the development of gastric metaplasia known as spasmolytic peptide-expressing metaplasia (SPEM),[12–14] which may be a precursor to gastric cancer.[15]

In mice, transgene-driven expression of IFN-γ in the brain leads to robust induction of the Hh pathway ligand/activator Sonic hedgehog (Shh). This deregulated activation of the Hh signaling pathway in turn leads to the development of medulloblastoma,[16,17] an Hh pathway–driven brain tumor. Because elevated activity of the Hedgehog (Hh) signaling pathway has also been linked to gastric cancer,[18,19] these results raised the interesting possibility that IFN-γ may contribute to inflammation-associated gastric neoplasia in part through induction of Shh expression and oncogenic signaling activity.

We tested the potential role of IFN-γ as a pivotal cytokine driving neoplastic progression in stomach by generating transgenic mice, designated *H/K-IFN-γ*, which overexpress murine *IFN-γ* driven by an H/K ATPase β promoter, which targets transgene expression to the gastric corpus. We show that *IFN-γ* overexpression leads to inflammation, increased proliferation, parietal cell and chief cell atrophy, SPEM, an increased number of myofibroblasts, dysplasia, and, in a subset of mice, tumor development. Interestingly, while this work was underway, another group produced mice with stomach-targeted overexpression of IFN-γ. Those mice, in which IFN-γ signaling was activated at lower levels than the mice described here, did not exhibit gastritis and SPEM. Indeed, these processes, as well as neoplasia driven by *Helicobacter* infection or IL-1β overexpression, were blocked.[20] In striking contrast, we show that robust expression of *IFN-γ* in our model is sufficient to orchestrate multiple changes in inflammatory, epithelial, and mesenchymal cell populations to drive premalignant progression in stomach, though additional alterations appear to be required for the development of full-blown neoplasia.

Materials and Methods

Transgenic Mice and Helicobacter felis *Infection*

Mouse *IFN-γ* cDNA was amplified from IMAGE clone ID 8733812 using forward primer 5′-CTACCTGACTGGATCCTCTGAGACAATGAACGCTAC-3′ and reverse primer 5′-GGAGTCGCTGCTGATTCGGATCCTTGACACATC-3′ and subcloned into the BamHI site to replace the Ctox cDNA in the *H/K-Ctox* transgene,[21] which contains 1059 bp of mouse H/K ATPase β promoter.[22] The resulting *H/K-mIFN-γ* transgene was verified by DNA sequencing, excised from vector with HindIII and SacII, and submitted to the University of Michigan Transgenic Animal Model Core for microinjection into F2 embryos from SJL × C57BL/6 parents. Eleven *H/K-mIFN-γ* founders were produced, and three exhibited severe SPEM associated with other histopathological changes. We studied mouse lines from founders 944 (*H/K-IFN-γ*^{944}) and 53 (*H/K-IFN-γ*^{53}), with most data generated from line *H/K-IFN-γ*^{944}. Transgenic mice were backcrossed onto a C57BL/6J background (The Jackson Laboratory, Bar Harbor, ME). For *Helicobacter felis* infections, 2-month-old C57BL/6J mice were gavaged three times over 3 days with 10^8 bacteria (CS1 strain), in 100 μL of *Brucella* broth.

Histopathological Scoring

Stomachs were cut along the greater curvature, placed on filter paper, fixed in 4% buffered paraformaldehyde overnight at 4°C, cut into strips extending from the forestomach to the proximal duodenum, and transferred to 70% ethanol until processing and paraffin embedding. Sections (5 μm) were stained using hematoxylin and eosin (H&E) and examined by a board-certified veterinary pathologist (K.A.E.) blinded to the experimental groups. Scoring was performed to quantify the presence of inflammation, SPEM, parietal and chief cell atrophy, gland atrophy, dysplasia, and tumor development. Histological scoring was performed on a scale of 0 to 3; 0, absence of detectable inflammation; 1, multiple focal areas of inflammation confined to the lamina propria; 2, inflammation that was widespread and/or that extended to the submucosa; and 3, transmural infiltration. For quantification of SPEM, the absence of detectable SPEM was scored as 0; mild or multifocal SPEM was scored as 1; the presence of SPEM in most fields was scored as 2; and widespread SPEM in all fields was scored as 3. Loss (atrophy) of parietal and chief cells was graded as 0, no loss; loss of cells detected was graded as 1; cell loss easily identified was graded as 2; and severe loss with few parietal or chief cells remaining was graded as 3. Gland atrophy was scored according to the appearance of the glands: 0, no change; 1, small or thin glands; 2, decreased gland size with space between glands; and 3, glands widely spaced with many missing. Dysplasia was scored as positive if there was cellular atypia with disorganized glands. Elderly *H/K-IFN-γ* mice occasionally developed more advanced lesions in their antra. Lesions that were focal but largely sessile, well differentiated, and had minimal dysplasia were interpreted as polyps. One focal proliferative lesion with marked dysplasia was interpreted as an adenoma. A single lesion with marked dysplasia, cellular atypia, and a high mitotic index was interpreted as an adenocarcinoma. For data comparing phenotypes in the corpus and antrum, inflammation and hyperplasia were scored as described above, and dysplasia was scored as follows: 0, no gland or cellular atypia; 1, the presence of occasional disorganized glands; 2, the presence of many disorganized glands; and 3, cellular atypia or expansile lesion.

Immunostaining, Antibodies, and Flow Cytometry

Immunohistochemical analysis was performed as previously described,[23] with minor modifications. Primary antibodies detecting the following antigens were used for immunostaining: mucin 5AC (#MS-145; NeoMarkers, Fremont, CA); H/K-ATPase α subunit (#D031-3; Medical and Biological Laboratories, Nagoya, Japan); intrinsic factor (a gift from Dr. David Alpers; Washington University, St. Louis, MO); Ki-67 (#RM-9106; Thermo Scientific, Fremont, CA); cleaved caspase 3 (D175, #9661; Cell Signaling, Danvers, MA); CD45 (#14–0451; eBioscience, San Diego, CA); CD3 (#A0452; DakoCytomation, Glostrup, Denmark); F4/80 (#T-2006; BMA Biomedicals, Augst, Switzerland); myeloperoxidase (#N1578; DakoCytomation); STAT1 (#ab31369; Abcam, Cambridge, MA); pSTAT1 (Y701) (#9167; Cell Signaling); pSTAT3 (Y705) (#9145; Cell Signaling); β-catenin (#C7207; Sigma-Aldrich, St. Louis, MO); TFF2 (anti-spasmolytic polypeptide antibody, #ab49536; Abcam); smooth muscle actin (SMA) (#MS-113-P0; NeoMarkers); keratin 5 (AF138, #PRB-160P; Covance, Princeton, NJ); keratin 8 (TROMA-I; DSHB, Iowa City, IA); and IFN-γRβ (Ifngr2) (N-20, #sc-971; Santa Cruz, Santa Cruz, CA). Fluorescein-conjugated GSII lectin (Vector Laboratories, Burlingame, CA) was used to identify mucous-containing neck cells in normal stomach and SPEM in *H/K-IFN-γ* transgenic mice. The following antibodies were used for immunoblotting: PCNA (#RB-9055; Thermo Scientific); Shh (#sc-1194; Santa Cruz); H/K-ATPase β subunit (#D032-3; Medical and Biological Laboratories); cleaved Caspase 3 (#9661; Cell Signaling); and GAPDH (#sc-25778; Santa Cruz). Flow cytometry was performed as previously described,[24] with minor modifications. Antibodies for sorting included PE rat anti-mouse Ly-6G and Ly-6C (Gr1) (#561084; BD Biosciences Pharmingen, San Diego, CA) and PE-Cy7 rat anti-mouse CD11b (#561098; BD Biosciences Pharmingen).

Immunoblot Analysis

Mucosal scrapings from freshly harvested stomach were homogenized for 20 minutes on ice by vortexing every 5 minutes in ice-cold radioimmunoprecipitation assay (RIPA) lysis buffer containing phosphatase inhibitor cocktail and protease inhibitor cocktail, both from Roche Applied Science (Indianapolis, IN). Lysates were cleared by centrifugation at 12,000 $\times$ *g* for 15 minutes at 4°C, aliquoted, and stored at −80°C. A 50-μg quantity of protein per lane was separated by gradient SDS–polyacrylamide gel electrophoresis and transferred onto a polyvinylidene fluoride membrane. Immunoblotting and detection were performed as described,[23] with minor modifications.

RT-qPCR Analysis

Stomach tissue samples were obtained from three to six independent mice per group, as described in the text, and frozen in RNAlater (Qiagen, Hilden, Germany). Total RNA was extracted using an RNeasy Mini Kit (Qiagen); single-stranded complementary DNA was synthesized using 2 μg of total RNA with SuperScript III Reverse Transcriptase (Invitrogen, Carlsbad, CA), and 2 μL of a 1:5 dilution of cDNA was used in a 20-μL quantitative RT-PCR reaction mix containing 2 μL of SYBR Green (1:10,000 dilution; #S-7563; Invitrogen), 100 nmol/L of each primer, 20 nmol/L fluorescein (#170–8780; Bio-Rad, Hercules, CA), 0.1 μL Platinum Tag polymerase (#10966–034, Invitrogen), and ultrapure water (#10977; Invitrogen). Primer sequences are available upon request. Real-time quantitation was performed in triplicate for each sample using the iCycler iQ5 Real-Time PCR System (Bio-Rad) and normalized to glyceraldehyde-3-phosphate dehydrogenase. Results are expressed as relative increase in the level of gene expression, compared to controls, using the threshold cycle (Ct) slope method.

Statistical Analysis

Statistical analysis was performed using GraphPad Prism (version 5) software. Statistical significance was determined using the two-tailed, unpaired, Student's *t*-test. Data are expressed as mean ± SEM. A *P* value of less than 0.05 was considered significant. Comparison of phenotypic scores for inflammation, hyperplasia, and dysplasia, in the corpus and antrum, was performed using Spearman's rank correlation coefficient. For quantification of histological changes over time, a Wilcoxon-Mann-Whitney test (nonparametric) was run with a multiple comparison *P* value adjustment.

Results

Production of Stomach-Targeted H/K-IFN-γ *Transgenic Mice*

To determine the consequences of *IFN-γ* overexpression in stomach, we generated transgenic mice using a 1059-bp fragment of the H/K ATPase β subunit promoter[22] to target mouse *IFN-γ* to gastric parietal and preparietal cells (Figure 1A). We focused our analysis on transgenic mouse lines derived from two founders, designated *H/K-IFN-γ^{944}* and *H/K-IFN-γ^{53}*. Gastric corpus isolated from both lines of mice exhibited elevated expression of IFN-γ mRNA, with levels in the *H/K-IFN-γ^{944}* line substantially higher than the *H/K-IFN-γ^{53}* line (Figure 1B). Expression of *IFN-γ* target genes *Mig* (*Cxcl9*) and *IP10* (*Cxcl10*) was also elevated (Figure 1C), indicating that *IFN-γ* overexpression elicited the expected transcriptional response. IFN-γ mRNA in *H/K-IFN-γ^{944}* mice was maintained at comparably high levels at 7 weeks and 15 months of age, whereas 15-month-old *H/K-IFN-γ^{53}* mice expressed reduced levels of IFN-γ relative to 7 weeks, and this was reflected in reduced expression of IFN-γ target genes (Figure 1, B and C).

To estimate whether the level of IFN-γ signaling in our mice was in the same range as in the setting of

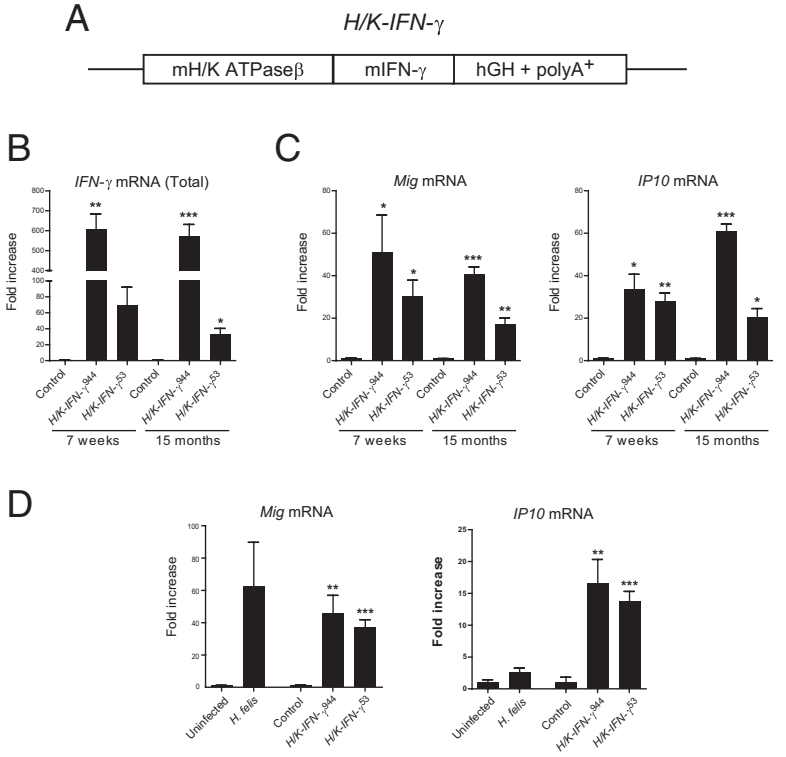

Figure 1. IFN-γ overexpression in stomach leads to sustained upregulation of IFN-γ target genes *Mig* and *IP10*. **A:** Transgene design, which includes mouse H/K ATPaseβ promoter sequence, mouse IFN-γ cDNA, and human growth hormone (hGH) sequence including intron and polyA$^+$ signal. **B:** Fold-increase of IFN-γ mRNA expression in corpus of *H/K-IFN-γ* transgenic mouse lines, relative to age-matched controls, at 7 weeks and 15 months of age. **C:** Fold-increase of IFN-γ target genes *Mig* and *IP10* in *H/K-IFN-γ* mouse lines relative to controls. Independent samples were obtained from three control, three *H/K-IFN-γ*^{944} mice and six *H/K-IFN-γ*^{53} mice. **D:** Fold-increase of IFN-γ target genes *Mig* and *IP10* in *H. felis*–infected versus uninfected mice, and *H/K-IFN-γ* transgenic mice versus control mice. Analysis was performed on six uninfected, seven *H. felis*-infected, four control, four *H/K-IFN-γ*^{944}, and four *H/K-IFN-γ*^{53} mice. All samples were collected from mice between 8 and 8.5 months of age, with *H. felis* infection at 2 months of age. Values are presented as mean ± SEM. Statistical significance relative to age-matched control or uninfected mice: $^*P < 0.05$, $^{**}P < 0.01$, and $^{***}P < 0.001$.

gastritis, we compared the expression of IFN-γ target genes in stomachs of *H. felis*–infected mice and *H/K-IFN-γ* mice, relative to controls. Mig mRNA expression levels, relative to controls, were elevated 63-fold in *H. felis*–infected mice, 46-fold in H/K- IFN-γ^{944} mice, and 37-fold in H/K- IFN-γ^{53} mice (Figure 1D). For the IFN-γ target gene IP10, expression levels relative to controls were elevated 2.6-fold in *H. felis*–infected mice, 17-fold in H/K-IFN-γ^{944} mice, and 14-fold in H/K-IFN-γ^{53} mice (Figure 1D). Taken together, these data support the notion that the level of IFN-γ signaling in *H/K-IFN-γ* transgenic mice, assessed by the expression level of IFN-γ target genes, is generally comparable to that observed in *H. felis*–infected mice.

Grossly, the stomachs from both lines of mice revealed a thickened and enlarged corpus region, and more than 50% of transgenic mice also exhibited thickening of the squamous limiting ridge at the junction of the forestomach and corpus (Figure 2A, arrow; see also Supplemental Figure S1 at *http://ajp.amjpathol.org*). Interestingly, 38% of mice from line 53 also contained areas of ectopic squamous epithelium within the glandular corpus (Figure 2A, arrowheads; see also Supplemental Figure S1 at *http://ajp.amjpathol.org*). This was not detected in control or *H/K-IFN-γ*^{944} mice. Stomach weights from *H/K-IFN-γ* mice were higher than those from control mice at all time points examined (Figure 2B), and there was an approximately twofold increase in mucosal thickness of the corpus at both 5 and 15 months of age (Figure 2C). Overexpression of *IFN-γ* in the corpus of transgenic mice thus leads to sustained elevation of transcripts encoding IFN-γ and IFN-γ target gene transcripts; this is associated with gastric hypertrophy, focal squamous hyperplasia, and, in one line of mice, ectopic squamous tissue within the corpus.

Parietal Cell Atrophy and Spasmolytic Peptide-Expressing Metaplasia in H/K-IFN-γ *Transgenic Mice*

Stomachs from *H/K-IFN-γ* transgenic mice revealed regions with marked histological changes involving multiple gastric cell types as well as a prominent inflammatory infiltrate. *H/K-IFN-γ* mice contained strikingly fewer parietal cells and chief cells, which were replaced by cells with abundant, foamy cytoplasm resembling the morphology of metaplastic cells comprising SPEM (Figure 3, A and B), a putative preneoplastic lesion both in humans and in mice.[15] Histopathological scoring of stomachs collected from control and *H/K-IFN-γ* mice at different ages quantified the presence of SPEM, parietal and chief cell atrophy, gland atrophy, and inflammation (Figure 3C), as described in *Materials and Methods*. Each of these histological features was either not detected or minimal in control mice but markedly altered in *H/K-IFN-γ* mice (Figure 3C).

The foamy cells in stomachs of *H/K-IFN-γ* transgenic mice contained abundant mucin identified by staining with PAS-Alcian blue (Figure 4, A and B), bound GSII lectin (Figure 4, C and D), and expressed TFF2 (Figure 4, E and F), supporting a diagnosis of SPEM. Expression of the mucous pit marker, Muc5ac, was generally reduced (Figure 4, G and H). Immunostaining for the α subunit of H/K ATPase (H/K ATPase α) revealed both a striking reduction in the number of parietal cells (Figure 4, I and J), in keeping with

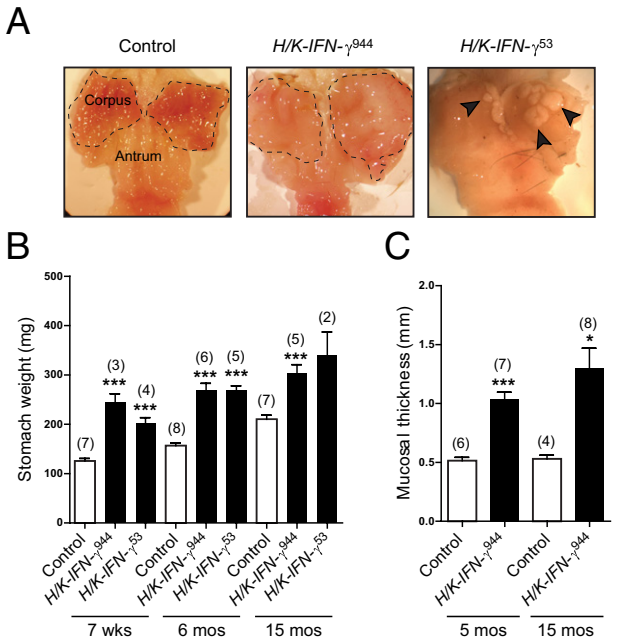

Figure 2. IFN-γ overexpression in stomach results in a sustained increase in stomach weight and mucosal thickness. **A:** Grossly thickened and expanded corpus (dashed line) of representative *H/K-IFN-γ*^{944} transgenic mouse at 15 months of age compared to control. Stomach from *H/K-IFN-γ*^{53} transgenic mouse at 11 months of age contains multiple foci of ectopic squamous epithelium in corpus (**arrowheads**). **B:** Increase in weight of stomachs from *H/K-IFN-γ* transgenic mice relative to controls. **C:** Quantification of increase in corpus mucosal thickness from *H/K-IFN-γ*^{944} transgenic mice. In **B** and **C**, number of animals per group is indicated in parentheses, and data are presented as mean ± SEM (or range for single data point with two mice). Statistical significance relative to age-matched control mice: $^{*}P < 0.05$, $^{**}P < 0.01$, $^{***}P < 0.001$.

the histopathological scoring (Figure 3C). Similarly, the number of cells expressing the chief cell marker, intrinsic factor, was also greatly reduced (Figure 4, K and L). In contrast, there was a marked expansion of mesenchymal cell expressing smooth muscle actin (SMA) (Figure 4, M and N), a marker of myofibroblasts.

IFN-γ Expression in Stomach Leads to Increased Proliferation and Cell Death

Additional immunostaining revealed increased proliferation in the corpus of *H/K-IFN-γ* transgenic mice. In contrast to control mice, where expression of the proliferation marker Ki-67 is largely restricted to a narrow band of cells within the isthmus region of each gastric gland, in *H/K-IFN-γ* mice there was both an increase in the number of Ki-67–positive cells and a broader distribution, with expansion deeper into gastric glands and more superficially (Figure 5, A–D). Co-immunostaining for Ki-67 and lineage markers revealed that proliferating cells in *H/K-IFN-γ* mice did not express Muc5ac (Figure 5, E and F) or H/K ATPase β (Figure 5, G and H), but some cells that bound GSII lectin were also Ki-67 positive (Figure 5, I and J). Thus, although neither the differentiated mucous pit nor the parietal cells are induced to proliferate in response to stomach-targeted expression of *IFN-γ*, a subset of metaplastic cells do express Ki-67.

In addition to enhanced proliferative activity, immunostaining for cleaved caspase 3 revealed increased apoptosis in the corpus of *H/K-IFN-γ* transgenic mice, and occasionally these cells were also positive for H/K ATPase β (Figure 5, K–N), suggesting that the loss of parietal cells is due at least in part to increased cell death. Immunoblotting studies examining markers of proliferation, differentiation, and cell death confirmed immunostaining results. Mucosal lysates from corpus of *H/K-IFN-γ* transgenic mice contained higher levels of PCNA and cleaved caspase 3, with reduced levels of the H/K ATPase β subunit and Sonic hedgehog (Shh) (Figure 5O), both of which are expressed in normal parietal cells, relative to controls.

We performed immunostaining to localize the expression pattern of the β subunit of the IFN-γ receptor, Ifngr2, in control and *H/K-IFN-γ* transgenic mice (see Supplemental Figure S2 at *http://ajp.amjpathol.org*). We co-immunostained with fluorescent GSII lectin, as a recent study reported that Ifngr2 is localized to mucous neck cells.[25] In control mice, Ifngr2 co-localizes with GSII lectin but also stains most cells in the lower portion of the

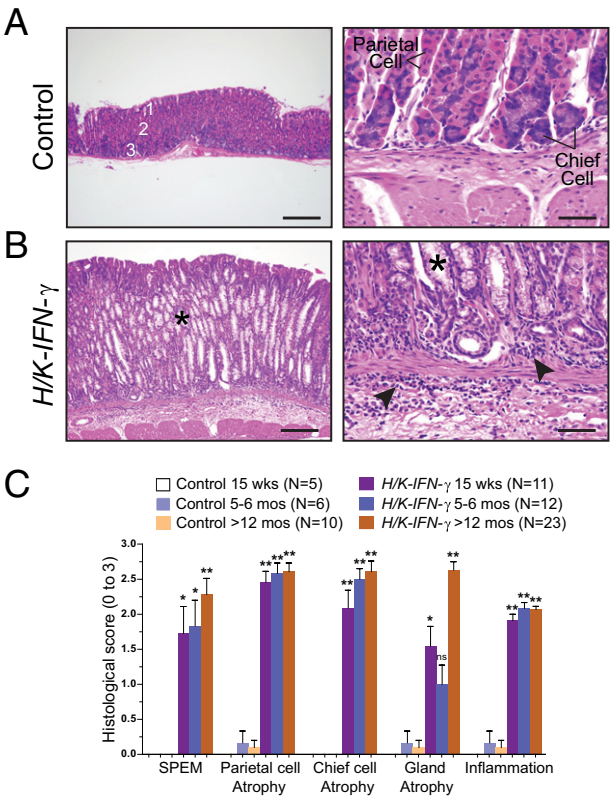

Figure 3. Parietal cell atrophy, inflammation, and mucous metaplasia in *H/K-IFN-γ* mice. **A** and **B:** H&E-stained sections of corpus from 5-month-old control and *H/K-IFN-γ* transgenic mice. **A:** Gastric glands in control corpus are subdivided into surface, neck, and base regions, containing mucous pit (1), parietal (2), and chief (3) cells. **B:** In *H/K-IFN-γ* mice, parietal and chief cells are largely replaced by foamy-appearing metaplastic cells (SPEM) (**asterisks**) and prominent inflammation is present in the lamina propria and submucosa (**arrowheads**). **C:** Quantification of the indicated histological changes (scores ranging from 0 to 3, as described in *Materials and Methods*) over time. The number of animals per data point is indicated in parentheses. Data are presented as mean ± SEM, with statistical significance relative to control mice at $^{*}P < 0.05$, $^{**}P < 0.01$, and $^{***}P < 0.001$. Scale bars: 100 μm (**left panels**); 20 μm (**right panels**).

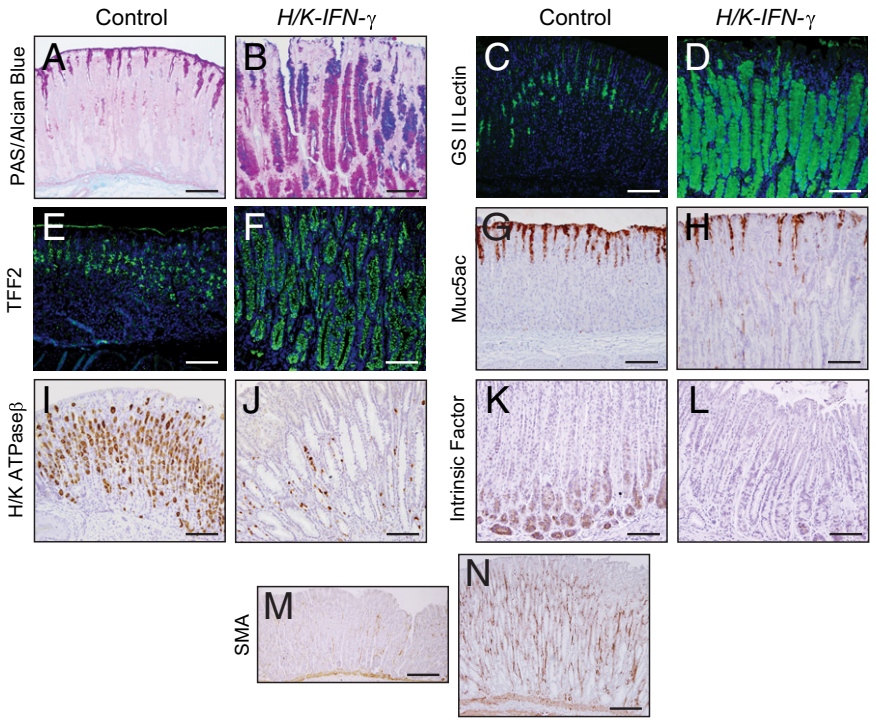

Figure 4. Alterations in gastric cell lineages in *H/K-IFN-γ* mice. **A** and **B:** PAS–Alcian Blue stain reveals massive expansion of mucin-containing cells, which also bind GS II lection (**C** and **D**) and immunostain with anti-TFF2 (**E** and **F**) in *H/K-IFN-γ* mouse corpus. Cells that bind GS II lectin and express TFF2 in control stomach are mucous neck cells. (**G** and **H**) Cells expressing the mucous pit cell marker Muc5ac are detected at reduced levels in *H/K-IFN-γ* mice. Parietal cells, identified by H/K ATPaseα immunostaining (**I** and **J**), and chief cells, immunostained for intrinsic factor (**K** and **L**), are reduced or absent in *H/K-IFN-γ* mice. The number of cells expressing the myofibroblast marker SMA (**M** and **N**) is increased in *H/K-IFN-γ* mice. Scale bars: 100 μm (**A–L**); 200 μm (**M** and **N**).

oxyntic glands in the gastric corpus, where chief cells are localized. In *H/K-IFN-γ* transgenic mice, epithelial expression of Ifngr2 is reduced or absent in regions with pronounced SPEM, and only a small subset of metaplastic GSII+ cells express appreciable levels of Ifngr2, in contrast to GSII+ mucous neck cells in the control stomach. Although Ifngr2 expression is reduced in regions with SPEM, it is not possible to ascertain in this setting whether this is due to chronic stimulation by IFN-γ with down-regulation of IFN-γ receptors, or to loss of some of the normal cell type(s) that express these receptors. Interestingly, scattered Ifngr-expressing cells are detected

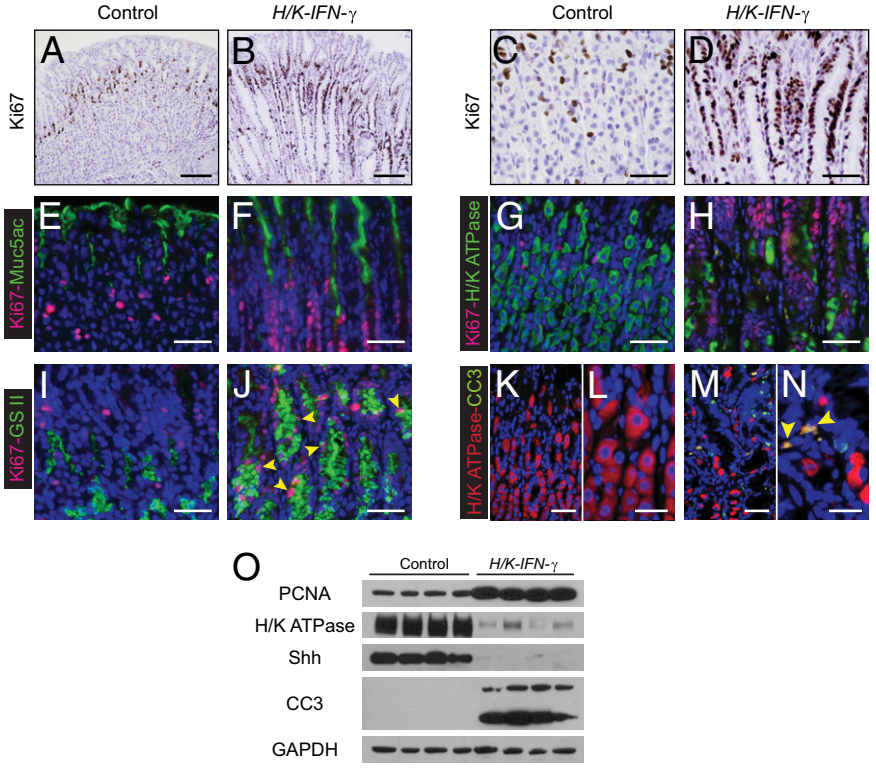

Figure 5. Expansion of proliferative cell compartment and increased apoptosis in *H/K-IFN-γ* mice. **A–D:** Ki-67 immunostaining. Identification of cycling, Ki-67–expressing cells in control (**A** and **C**) and *H/K-IFN-γ* mice (**B** and **D**) reveals marked expansion of the proliferative zone in *H/K-IFN-γ* mice. **E–J:** Double-immunostaining for Ki-67 and lineage markers. Proliferating cells in *H/K-IFN-γ* mice do not express the mucous pit marker Muc5ac (**E** and **F**) or parietal cell marker H/K ATPase (**G** and **H**), but a subset of Ki-67–expressing cells binds GSII lectin (**I** and **J, arrowheads**). **K–N:** Co-immunostaining reveals that a subset of H/K ATPase-expressing cells in *H/K-IFN-γ* mice also express the apoptosis marker cleaved caspase 3 (CC3) (**N, arrowheads**). **O:** Immunoblotting using corpus lysates shows upregulation of PCNA, reduction of H/K ATPase and Shh (parietal cell markers), and increased expression of the apoptosis marker CC3 (**lower band**). Scale bars: 100 μm (**A** and **B**); 40 μm (**C–J, K,** and **M**); 20 μm (**L** and **N**).

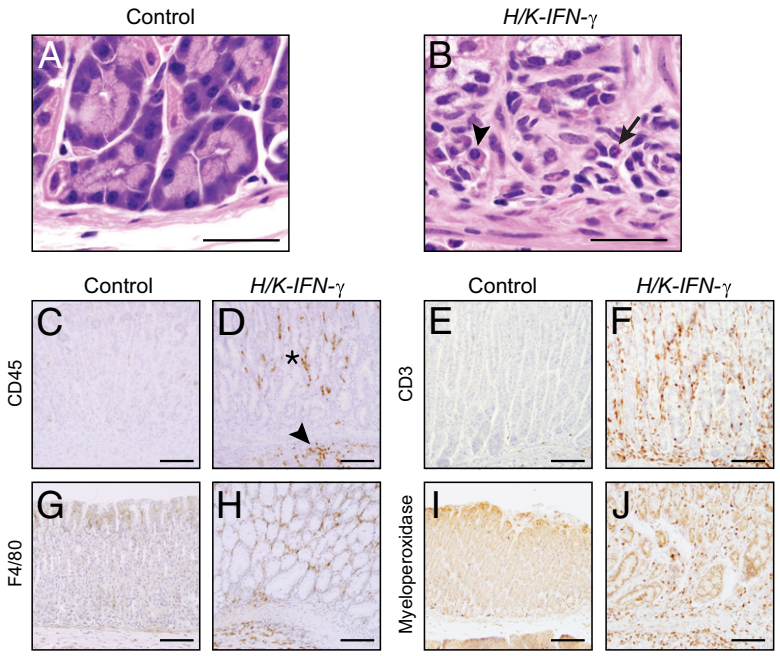

Figure 6. Mixed inflammatory infiltrate in corpus of *H/K-IFN-γ* mice. **A** and **B:** Inflammatory infiltrate in corpus of *H/K-IFN-γ* mouse showing mononuclear cells, plasma cells (**arrowhead**), and neutrophils (**arrow**). **C** and **D:** Anti-CD45 immunostaining confirms the presence of leukocytes in the lamina propria (**asterisk**) and submucosa (**arrowhead**) of the gastric corpus of a *H/K-IFN-γ* mouse. T cells are identified by anti-CD3 (**E** and **F**), macrophages by anti-F4/80 (**G** and **H**), and neutrophils by anti-myeloperoxidase (**I** and **J**) immunostaining. Scale bars: 30 μm (**A** and **B**); 100 μm (**C–J**).

in regions of corpus of *H/K-IFN-γ* mice, and these appear to be nonepithelial (see Supplemental Figure S2 at *http://ajp.amjpathol.org*).

IFN-γ Overexpression in Stomach Has Biphasic Effects on Hedgehog Signaling Activity

Although early stages of gastric tumorigenesis are characterized by reduced Shh levels and lowered Hh pathway activity, likely due largely to the loss of the Shh-expressing parietal cells, progression to gastric cancer is associated with elevated levels of Hh ligands and signaling activity.[26,27] The reduced level of Shh protein in *H/K-IFN-γ* mice (Figure 5O) was associated with lower Hh pathway activity in regions with prominent SPEM, detected by x-gal staining of stomachs from 10-week-old *H/K-IFN-γ;Gli1-lacZ* Hh target gene reporter mice (see Supplemental Figure S3 at *http://ajp.amjpathol.org*). Quantitative PCR at 7 weeks of age revealed similar levels of mRNA encoding Shh, Indian hedgehog (Ihh), and the Hh target genes *Gli1* and *Hhip* in the corpus of *H/K-IFN-γ* and control mice, with the target gene *Ptch1* expressed at lower levels in *H/K-IFN-γ*^{944} mice than in controls (see Supplemental Figure S3 at *http://ajp.amjpathol.org*). At 15 months of age, however, statistically significant increases were noted in the expression of *Shh* and *Ihh*, as well as *Ptch1* and *Hhip*, in *H/K-IFN-γ* transgenic mice relative to controls (see Supplemental Figure S3 at *http://ajp.amjpathol.org*).

Robust Inflammation, Cytokine Induction, and Activation of STAT1 and STAT3 in H/K-IFN-γ *Transgenic Mice*

Inflammatory cells in H&E-stained sections of *H/K-IFN-γ* mice were distributed in regions throughout the corpus in the mucosa and occasionally submucosa (Figure 3, A and B), and contained variable amounts of mononuclear cells, including plasma cells, and neutrophils (Figure 6, A and B). Immunostaining to detect CD45 confirmed increased numbers of leukocytes in the corpus of *H/K-IFN-γ* transgenic mice (Figure 6, C and D). The infiltrate included T lymphocytes (CD3-positive) (Figure 6, E and F), macrophages (F4/80 antigen-positive) (Figure 6, G and H), and neutrophils (myeloperoxidase-positive) (Figure 6, I and J).

The robust inflammation in *H/K-IFN-γ* mice was accompanied by elevated expression of mRNAs encoding markers for distinct subsets of T cells and multiple cytokines, measured at both 7 weeks and 15 months of age. Quantitative PCR revealed upregulation of transcripts encoding T helper cell markers T-bet and Foxp3, markers of Th1[28] and Treg[29] cells, respectively (Figure 7). In addition, *H/K-IFN-γ* mice expressed elevated levels of transcripts encoding the Th1-related cytokines tumor necrosis factor–α (TNF-α) and IL-12 (p40); as well as the Treg-related anti-inflammatory cytokine IL-10 (Figure 7). Transcripts encoding the pro-inflammatory cytokines IL-1β and IL-6, both implicated in tumorigenesis in stomach, were also upregulated (Figure 7). IL-11 was significantly elevated in *H/K-IFN-γ*^{944} mice, but only at 15 months of age.

H/K-IFN-γ mice did not express significantly higher levels of mRNAs encoding the Th17 marker RORγT and Th17 cytokines IL-17A, IL-17B; Th17-related IL-23 (p19); Th1-related IL-12 (p35); and the Th2 marker Gata3 and Th2 cytokine IL-4 (see Supplemental Figure S4 at *http://ajp.amjpathol.org*). These findings are in keeping with the inhibitory effects of IFN-γ on Th2 and Th17 development. Overexpression of *IFN-γ* in mouse corpus thus activates a robust, sustained inflammatory response with a predominant Th1 profile. Interestingly, despite markedly higher levels of *IFN-γ* in *H/K-IFN-γ*^{944} than

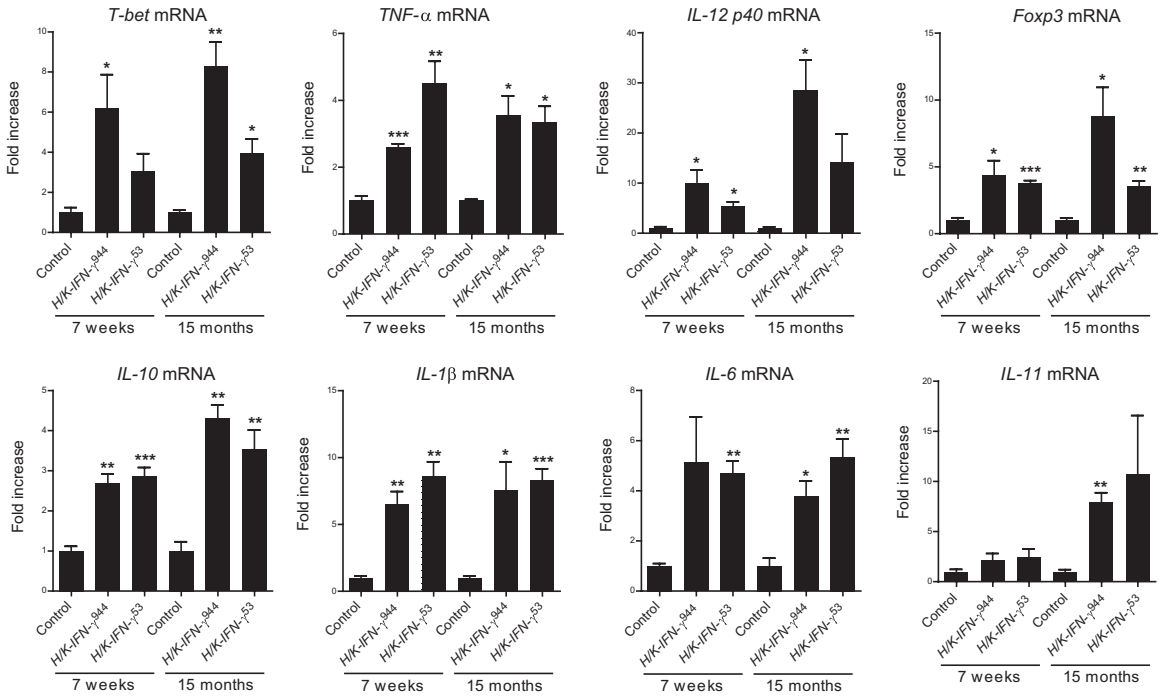

Figure 7. Prolonged elevation of pro-inflammatory cytokines in corpus of *H/K-IFN-γ* mice. Transcripts for the indicated T-cell subsets and cytokines were measured by quantitative PCR in RNAs isolated from control, *H/K-IFN-γ*^{944}, and *H/K-IFN-γ*^{53} mice, collected at 7 weeks and 15 months of age. *H/K-IFN-γ* mice expressed elevated levels of Th1 and regulatory T markers and cytokines, as well as IL-1β and IL-6. $N = 3$ for controls and *H/K-IFN-γ*^{944} mice and $N = 6$ for *H/K-IFN-γ*^{53} mice. Data are expressed as mean ± SEM, with statistical significance relative to age-matched controls at $^{*}P < 0.05$, $^{**}P < 0.01$, and $^{***}P < 0.001$.

H/K-IFN-γ^{53} mice (Figure 1B), upregulation of mRNA for most of the cytokines examined, including those previously implicated in gastric metaplasia and transformation (IL-6, TNF-α, and IL-1β), was generally comparable in both lines of *H/K-IFN-γ* mice (Figure 7). This suggests that a threshold sufficient for near-maximal signaling may have been reached even in the lower-expressing *H/K-IFN-γ*^{53} mice.

To test the requirement for acquired immunity in the phenotypic changes detected in *H/K-IFN-γ* mice, we generated mice deficient in B and T cells by breeding *H/K-IFN-γ* mice with mice carrying *Rag1* null alleles.[30] The histopathological score for *H/K-IFN-γ* and *H/K-IFN-γ; Rag1*$^{-/-}$ mice was not appreciably different (see Supplemental Figure S5 at *http://ajp.amjpathol.org*): epithelial changes and inflammation were present in both groups of mice. As expected, immunostaining for CD3 confirmed the absence of T-cells in *Rag1*$^{-/-}$ and *H/K-IFN-γ; Rag1*$^{-/-}$ mice (see Supplemental Figure S5 at *http://ajp.amjpathol.org*). These data show that the marked phenotypic changes seen in corpus of *H/K-IFN-γ* transgenic mice are not dependent on acquired immunity and reflect similar findings in H/K ATPase-targeted IL-1β-expressing mice, where T-cell function is dispensable but myeloid-derived suppressor cells (MDSCs) may play an important role in the development of gastritis and dysplasia.[11] In light of these findings, we performed flow cytometry to assess whether IFN-γ overexpression also leads to recruitment of MDSCs. As shown in Supplemental Figure S6 (available at *http://ajp.amjpathol.org*), the proportion of MDSCs in *H/K-IFN-γ*^{944} mouse stomach is 29-fold higher than in control mice (1.933% versus 0.0667%; $P < 0.0001$). There is also a 5.5-fold increase in MDSCs in *H/K-IFN-γ*^{53} mice (0.3667%), relative to controls (0.0667%), but this is not statistically significant (see Supplemental Figure S6 at *http://ajp.amjpathol.org*). These results are in keeping with the concept that infiltrating MDSCs may contribute to the phenotype that develops in *H/K-IFN-γ* transgenic mice, but additional studies would be needed to rigorously address this possibility.

Given the central role of signal transducers of transcription (STATs) in cellular responsiveness to cytokines, we examined the expression and phosphorylation/activation status of STAT1 and STAT3 in stomach of *H/K-IFN-γ* mice. Immunostaining for STAT1, pSTAT1, and pSTAT3 revealed very low expression of these signaling molecules in control stomach. In contrast, there was marked upregulation of these proteins in affected regions of corpus of *H/K-IFN-γ* transgenic mice (Figure 8, A–I). Co-immunostaining with the epithelial cell-surface marker β-catenin revealed pSTAT1 primarily in epithelial cells, whereas pSTAT3 was detected both in epithelial and in nonepithelial cells (Figure 8, J and K). Cells expressing pSTAT3 included parietal cells, GSII lectin-binding SPEM cells, and SMA-positive mesenchymal cells (Figure 8, L–T), indicating that STAT3 signaling is activated in stromal and multiple epithelia cell populations in *H/K-IFN-γ* mice. Immunostaining results for STAT1 and STAT3 proteins were corroborated by immunoblotting (Figure 8U).

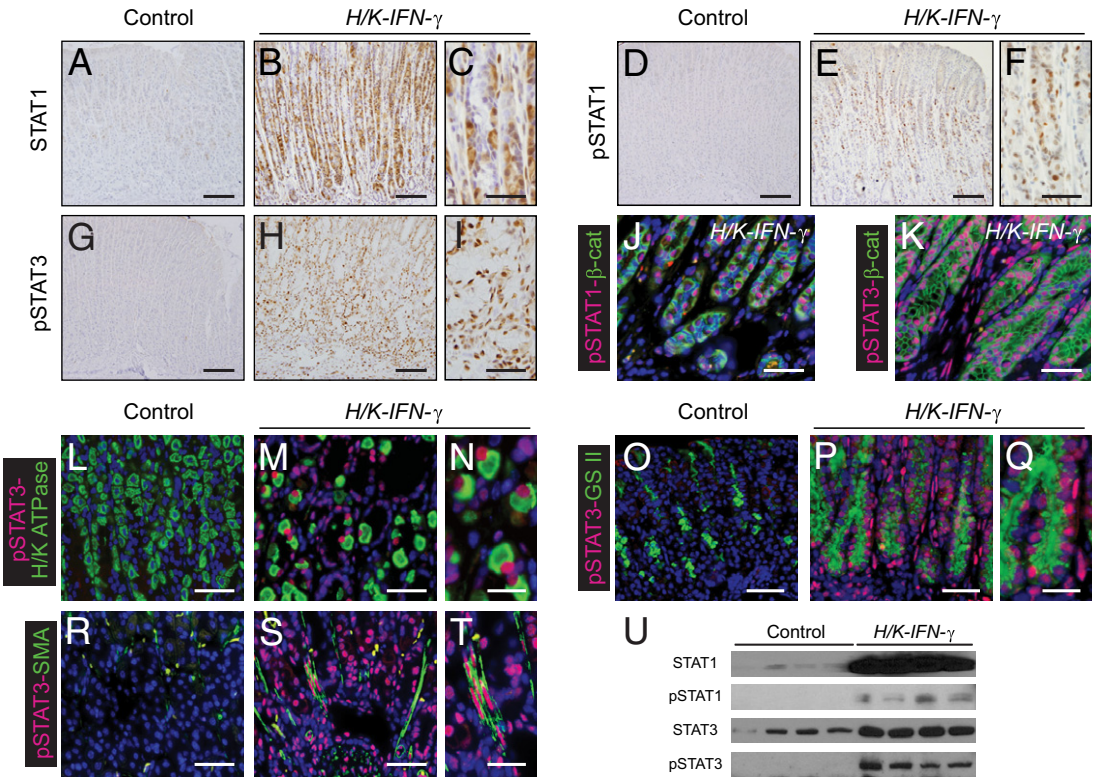

Figure 8. Activation of STAT1 and STAT3 in the corpus of *H/K-IFN-γ* mice. **A–C:** Immunostaining for STAT1 reveals marked upregulation in *H/K-IFN-γ* mouse with negligible expression in control stomach. Higher magnification in **C** shows a subset of cells with STAT1 localized to the nucleus. pSTAT1 (**D–F**) and pSTAT3 (**G–I**) are highly expressed in corpus of *H/K-IFN-γ* mice. Co-immunostaining for the epithelial marker β-catenin (β-cat) shows localization of pSTAT1 predominantly in epithelial cells (**J**), whereas pSTAT3 is detected in epithelial and nonepithelial (β-cat–negative) cell populations (**K**). Co-immunostaining with lineage markers reveals expression of pSTAT3 in parietal cells (**L–N**), GS II lectin-binding metaplastic cells (**O–Q**), and SMA-expressing mesenchymal cells (**R–T**) in *H/K-IFN-γ* mice. **U:** Immunoblot analysis supports results of immunostaining. Scale bars: 100 μm (**A, B, D, E, G,** and **H**); 40 μm (**C, F, I, J, K, L, M, O, P, R,** and **S**); 20 μm (**N, Q,** and **T**).

Preneoplastic Progression and Antral Tumor Development in H/K-IFN-γ *Transgenic Mice*

Because SPEM is considered a preneoplastic process and *H/K-IFN-γ* mice developed prominent and persistent SPEM, we were interested in assessing whether *H/K-IFN-γ* mice were at increased risk for developing gastric cancer. In addition to metaplasia and other histological changes quantified in Figure 3C, *H/K-IFN-γ* mice developed dysplasia, cystic gland dilatation with occasional herniation into the submucosa, and gastric gland atrophy (Figure 9, A–F). Dysplasia was common in *H/K-IFN-γ* mice: at 3 to 5 months of age, 46% of *H/K-IFN-γ*^{944} and 50% of *H/K-IFN-γ*^{53} mice exhibited areas of dysplasia; in mice over 12 months of age, 65% of *H/K-IFN-γ*^{944} and 44% of *H/K-IFN-γ*^{53} mice had regions of dysplasia (Figure 9F). In contrast, dysplasia was not detected in any of the control mice at similar ages (Figure 9F). The similar levels of dysplasia in *H/K-IFN-γ*^{944} and *H/K-IFN-γ*^{53} mice suggests that even the lower-expressing strain 53 produces sufficient IFN-γ to drive this preneoplastic change. This concept is supported by the comparable expression levels of IFN-γ target genes, as well as transcripts encoding multiple cytokines, in *H/K-IFN-γ*^{944} and *H/K-IFN-γ*^{53} mice (Figures 1 and 7).

Four of 39 (10%) *H/K-IFN-γ* mice over 1 year of age developed either polyps or more advanced lesions, and, interestingly, all of these were located in the antrum (Figure 9, G, H, J, and K). One *H/K-IFN-γ*^{944} mouse developed an antral adenoma at 18 months of age (Figure 9, G and H); two *H/K-IFN-γ*^{53} mice developed antral polyps, one at 14 months and another at 21 months of age; and one *H/K-IFN-γ*^{53} mouse developed an antral adenocarcinoma (Figure 9, J and K) at 21 months of age. This tumor was characterized by marked dysplasia, cellular atypia, and a high mitotic index. In addition, this tumor contained cells with β-catenin localized prominently to nuclei (see Supplemental Figure S7 at *http://ajp.amjpathol.org*), consistent with activated canonical Wnt/β-catenin signaling, which has previously been linked to gastric cancer development.[31,32] Despite the appearance of advanced lesions in transgenic but not control mice, this difference was not statistically significant (Fisher's exact test, $P = 0.32$).

The development of antral changes was nonetheless surprising, as IFN-γ expression in our mice was targeted to the gastric corpus. We therefore examined several parameters to look for any correlation between alterations in the corpus and the antrum. Interestingly, we found a moderate correlation for hyperplasia ($r = 0.45$; $P = 0.0003$) but no correlation for inflammation ($r = 0.12$; $P = 0.351$) or dysplasia ($r = 0.09$; $P = 0.474$) (see Supplemental Figure S8 at *http://ajp.amjpathol.org*). Additional studies will be required to gain insight into the mechanism underlying antral hyperplasia in this setting and its long-term consequences.

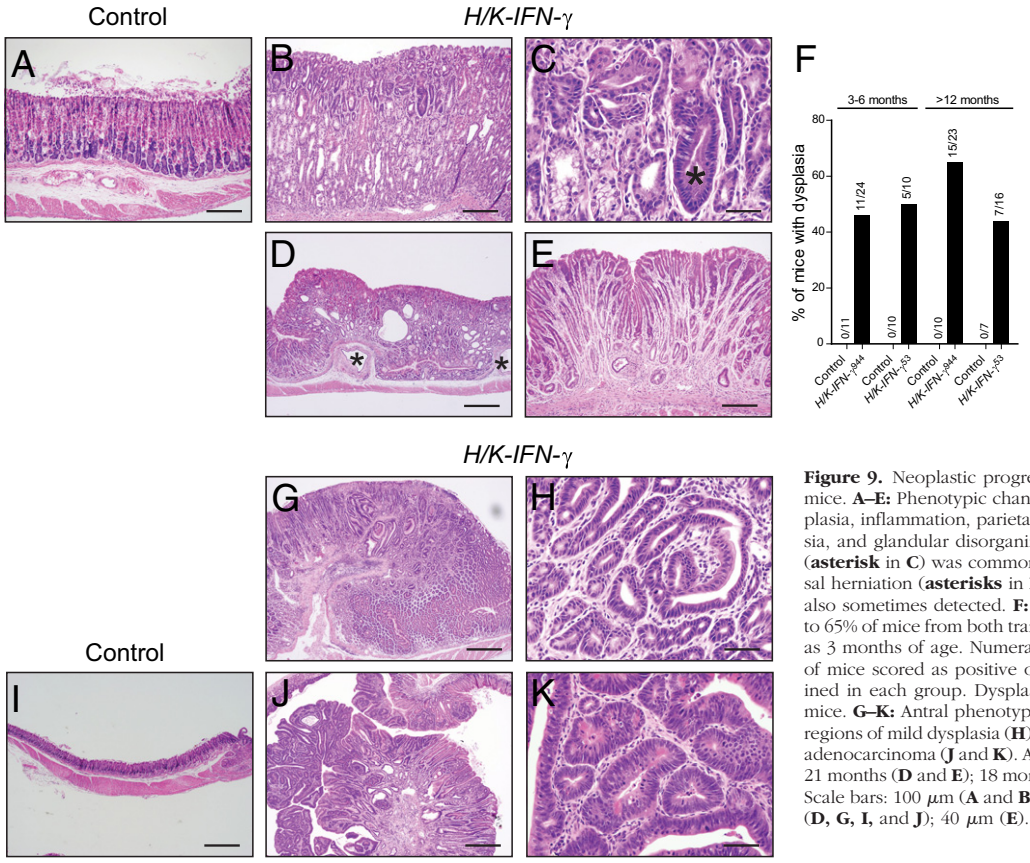

Figure 9. Neoplastic progression in stomach of *H/K-IFN-γ* mice. **A–E:** Phenotypic changes in the corpus include metaplasia, inflammation, parietal and chief cell atrophy, dysplasia, and glandular disorganization. Progression to dysplasia (**asterisk** in **C**) was common, and cystic dilation, submucosal herniation (**asterisks** in **D**), and gland atrophy (**E**) were also sometimes detected. **F:** Dysplasia was detected in 44% to 65% of mice from both transgenic lines, beginning as early as 3 months of age. Numerals above bars indicate numbers of mice scored as positive over the number of mice examined in each group. Dysplasia was not detected in control mice. **G–K:** Antral phenotypes included adenomas (**G**) with regions of mild dysplasia (**H**) or severe dysplasia and a single adenocarcinoma (**J** and **K**). Ages of mice: 20.5 months (**A–C**); 21 months (**D** and **E**); 18 months (**G–I**); 21 months (**J** and **K**). Scale bars: 100 μm (**A** and **B**); 20 μm (**C, H,** and **K**); 200 μm (**D, G, I,** and **J**); 40 μm (**E**).

Discussion

The results of this study establish that stomach-targeted overexpression of *IFN-γ* orchestrates histological changes associated with neoplastic progression that involve inflammatory, epithelial, and mesenchymal cell populations. Although *IFN-γ*-overexpressing mice develop dysplasia with high penetrance and occasionally develop more advanced lesions, only one *H/K-IFN-γ* mouse developed an adenocarcinoma. These data support the notion that although *IFN-γ* plays an important role during early stages of gastric tumorigenesis, additional alterations are required for the development of frank malignancy.

Our findings contrast with those reported by Tu and colleagues,[20] who generated *IFN-γ*-expressing mice using the same H/K ATPase β promoter fragment to drive transgene expression in the corpus. These investigators found no induction of inflammation or SPEM in their mice; rather, *Helicobacter* and IL-1β–driven inflammation and dysplasia were suppressed in their IFN-γ-overexpressing mice.[20] A likely explanation for the disparate results of these two studies may lie in the different levels of IFN-γ signaling in the two models: the relative increase in IFN-γ target gene expression in our mice was an order of magnitude higher than that reported in the earlier study, and in a similar range as seen in *H. felis*–infected mice (Figure 1). This was associated with upregulation of mRNAs encoding multiple pro-inflammatory cytokines, including IL-1β, TNF-α, and IL-6, at both 7 weeks and 15 months of age (Figure 7), none of which were upregulated at 12 months of age in the report by Tu and colleagues.[20]

We detected SPEM, inflammation, and other phenotypic changes in the corpus of H/K-IFN-γ mice (Figure 3), with dysplasia evident as early as 3 months of age (Figure 9). As they aged, *H/K-IFN-γ* mice developed dilated cystic glands that sometimes herniated into the submucosa (Figure 9). In addition to changes in the corpus, some aged mice (>12 months) developed more advanced lesions in the antrum, including one adenoma, two polyps, and an adenocarcinoma (Figure 9, G, H, J, and K). The nuclear β-catenin detected in the sole adenocarcinoma that developed in one of our mice (see Supplemental Figure S7 at *http://ajp.amjpathol.org*) argues that canonical Wnt/β-catenin signaling synergizes with *IFN-γ*, as it does with other signaling molecules,[11,32] to drive development of full-blown gastric cancer. Although the number of advanced lesions that develop in the antra of *H/K-IFN-γ* mice is not statistically increased over that of controls; their presence contrasts sharply with the lack of tumor development in the corpus, despite the presence of long-standing pre-neoplastic changes, and in some cases severe dysplasia (Figure 9, B–E), in this region of the stomach.

Quantitative mRNA analysis in our mice shows sustained expression of markers for both Th1 (*T-bet*) and Treg (*Foxp3*) T cell subsets, as well as both pro-inflammatory (TNF-α, IL-1β, and IL-6) and anti-inflammatory (IL-10) cytokines (Figure 7). Despite these findings, nei-

ther T nor B cells are required for the responses of gastric epithelium to IFN-γ, at least at early time points, as phenotypic scoring was similar in control and *Rag1*-deficient *H/K-IFN-γ* mice (see Supplemental Figure S5 at *http://ajp.amjpathol.org*). The increased proportion of MDSCs in *H/K-IFN-γ* mice (see Supplemental Figure S6 at *http://ajp.amjpathol.org*) raises the possibility that this cell population may contribute to preneoplastic changes in *H/K-IFN-γ* mice, as proposed by Wang and colleagues[11] in *H/K-IL-1β* mice.

Cytokine-mediated activation of the transcription factor Stat3 is emerging as a key driver of inflammation-associated tumorigenesis in several organs,[33–35] where it may be activated in epithelial, stromal, or inflammatory cells.[36] The importance of this pathway in stomach cancer is supported by the rapid appearance of gastric tumors in mice with a mutant form of the IL-6/IL-11 co-receptor gp130 ($gp130^{Y757F}$) leading to STAT3 activation,[37] and the correlation between gp130/STAT3 signaling and prognosis of human gastric cancer.[38] Despite robust pSTAT3 expression in multiple cell types seen in *H/K-IFN-γ* mice (Figure 8), activation of this key signaling effector is not sufficient to drive advanced stages of tumorigenesis in our model. Although IL-6 is the key cytokine driving oncogenic STAT3 signaling in pancreatic[39] and colitis-associated colon cancer,[40] IL-11 appears to be preferentially involved in activating STAT3 signaling in stomach.[41,42] IL-6 appears to be more consistently elevated than IL-11 in *H/K-IFN-γ* mice (Figure 7), but further studies will be needed to define the mechanism of STAT3 activation and its functional consequences in this model.

H/K-IFN-γ transgenic mice exhibited abnormalities involving squamous epithelia in stomach. Over 50% of mice from both transgenic lines developed squamous hyperplasia of the limiting ridge, whereas 6% or less developed squamous papillomas (see Supplemental Figure S1 at *http://ajp.amjpathol.org*). Most strikingly, 38% of *H/K-IFN-*γ^{53} mice, but none of the *H/K-IFN-*γ^{944} mice or controls, exhibited foci of squamous epithelium within the corpus (Figure 2A, and see Supplemental Figure S1 at *http://ajp.amjpathol.org*). Squamous metaplasia in the human stomach has been described rarely, typically in association with ulcers and/or inflammation,[43,44] and it may be a precursor lesion for the development of squamous cell carcinoma,[45,46] which was not detected in our mice. The appearance of ectopic squamous foci in only one of the two *H/K-IFN-γ* transgenic lines could indicate that the specific level of IFN-γ/inflammation present in line 53 is required for the development of this phenotype; but we cannot rule out the possibility that insertional mutagenesis has altered the function of a gene involved in epithelial cell fate specifically in the *H/K-IFN-*γ^{53} transgenic line.

Finally, the initial impetus for this project stemmed from studies showing that *IFN-γ* expression in cerebellum leads to Shh expression, Hh signaling activity, and the development of medulloblastoma,[16,17] raising the possibility that a similar scenario could lead to oncogenic Hh signaling and contribute to inflammation-associated gastric cancer. In keeping with this idea, IFN-γ directly activates Shh gene expression via STAT binding sites[47] and leads to upregulation of Shh in cultured canine parietal cells.[48] However, in relatively young *H/K-IFN-γ* mice (7 weeks), at a time when IFN-γ target genes are highly up-regulated (Figure 1), we find no evidence of increased Hh pathway activity (see Supplemental Figure S3 at *http://ajp.amjpathol.org*). This argues that the link between IFN-γ, elevated Shh expression, and tumorigenesis described in brain is likely not applicable to stomach. Moreover, in contrast to neuronal cells, IFN-γ appears to inhibit Hh signaling in white adipose tissue,[49] underscoring the divergent responses of different cell types to IFN-γ. In contrast to the results at 7 weeks of age, both lines of *H/K-IFN-γ* mice at 15 months expressed substantially higher levels of Hh ligands and Hh target genes than did age-matched controls (see Supplemental Figure S3 at *http://ajp.amjpathol.org*). Additional studies will be required to identify Hh-producing and Hh-responsive cells in this setting, and to ascertain their potential role in gastric pathology in aging *H/K-IFN-γ* mice.

In summary, we have shown that expression of IFN-γ in stomach is sufficient to drive a strong and sustained response involving inflammatory, mesenchymal, and epithelial cells with multiple features of pre-neoplasia. These findings strongly support the notion that inflammation plays a key role during early stages of gastric tumorigenesis but is dependent on additional alterations to drive cancer development, and suggest that targeting key pro-inflammatory cytokines may provide a useful approach to chemoprevention.

Acknowledgments

Helpful comments were provided by John Kao and Milena Saqui-Salces. We thank Heather Chubb for expert assistance with statistics, Margaret Van Keuren and Wanda Filipiak for preparation of transgenic mice, and the Transgenic Animal Model Core of the University of Michigan's Biomedical Research Core Facilities.

References

1. Jemal A, Bray F, Center MM, Ferlay J, Ward E, Forman D: Global cancer statistics. CA Cancer J Clin 2011, 61:69–90
2. Siegel R, Ward E, Brawley O, Jemal A: Cancer statistics, 2011: the impact of eliminating socioeconomic and racial disparities on premature cancer deaths. CA Cancer J Clin 2011, 61:212–236
3. Correa P, Piazuelo MB: Helicobacter pylori infection and gastric adenocarcinoma. US Gastroenterol Hepatol Rev 2011, 7:59–64
4. Parsonnet J, Friedman GD, Vandersteen DP, Chang Y, Vogelman JH, Orentreich N, Sibley RK: Helicobacter pylori infection and the risk of gastric carcinoma. N Engl J Med 1991, 325:1127–1131
5. Gonda TA, Tu S, Wang TC: Chronic inflammation, the tumor microenvironment and carcinogenesis. Cell Cycle 2009, 8:2005–2013
6. Grivennikov SI, Greten FR, Karin M: Immunity, inflammation, and cancer. Cell 2010, 140:883–899
7. Mantovani A, Allavena P, Sica A, Balkwill F: Cancer-related inflammation. Nature 2008, 454:436–444
8. Balkwill F, Mantovani A: Cancer and inflammation: implications for pharmacology and therapeutics. Clin Pharmacol Ther 2010, 87:401–406
9. El-Omar EM, Carrington M, Chow WH, McColl KE, Bream JH, Young HA, Herrera J, Lissowska J, Yuan CC, Rothman N, Lanyon G, Martin M, Fraumeni JF, Jr., Rabkin CS: Interleukin-1 polymorphisms associated with increased risk of gastric cancer. Nature 2000, 404:398–402

10. Machado JC, Pharoah P, Sousa S, Carvalho R, Oliveira C, Figueiredo C, Amorim A, Seruca R, Caldas C, Carneiro F, Sobrinho-Simoes M: Interleukin 1B and interleukin 1RN polymorphisms are associated with increased risk of gastric carcinoma. Gastroenterology 2001, 121:823–829
11. Tu S, Bhagat G, Cui G, Takaishi S, Kurt-Jones EA, Rickman B, Betz KS, Penz-Oesterreicher M, Bjorkdahl O, Fox JG, Wang TC: Overexpression of interleukin-1beta induces gastric inflammation and cancer and mobilizes myeloid-derived suppressor cells in mice. Cancer Cell 2008, 14:408–419
12. Sawai N, Kita M, Kodama T, Tanahashi T, Yamaoka Y, Tagawa Y, Iwakura Y, Imanishi J: Role of gamma interferon in Helicobacter pylori-induced gastric inflammatory responses in a mouse model. Infect Immun 1999, 67:279–285
13. Yamaoka Y, Yamauchi K, Ota H, Sugiyama A, Ishizone S, Graham DY, Maruta F, Murakami M, Katsuyama T: Natural history of gastric mucosal cytokine expression in Helicobacter pylori gastritis in Mongolian gerbils. Infect Immun 2005, 73:2205–2212
14. Roth KA, Kapadia SB, Martin SM, Lorenz RG: Cellular immune responses are essential for the development of Helicobacter felis-associated gastric pathology. J Immunol 1999, 163:1490–1497
15. Goldenring JR, Nam KT: Oxyntic atrophy, metaplasia, and gastric cancer. Prog Mol Biol Transl Sci 2010, 96:117–131
16. Lin W, Kemper A, McCarthy KD, Pytel P, Wang JP, Campbell IL, Utset MF, Popko B: Interferon-gamma induced medulloblastoma in the developing cerebellum. J Neurosci 2004, 24:10074–10083
17. Wang J, Pham-Mitchell N, Schindler C, Campbell IL: Dysregulated Sonic hedgehog signaling and medulloblastoma consequent to IFN-alpha-stimulated STAT2-independent production of IFN-gamma in the brain. J Clin Invest 2003, 112:535–543
18. Watkins DN, Peacock CD: Hedgehog signalling in foregut malignancy. Biochem Pharmacol 2004, 68:1055–1060
19. Ma X, Chen K, Huang S, Zhang X, Adegboyega PA, Evers BM, Zhang H, Xie J: Frequent activation of the hedgehog pathway in advanced gastric adenocarcinomas. Carcinogenesis 2005, 26:1698–1705
20. Tu SP, Quante M, Bhagat G, Takaishi S, Cui G, Yang XD, Muthuplani S, Shibata W, Fox JG, Pritchard DM, Wang TC: IFN-[gamma] inhibits gastric carcinogenesis by inducing epithelial cell autophagy and T-cell apoptosis. Cancer Res 2011, 71:4247–4259
21. Lopez-Diaz L, Hinkle KL, Jain RN, Zavros Y, Brunkan CS, Keeley T, Eaton KA, Merchant JL, Chew CS, Samuelson LC: Parietal cell hyperstimulation and autoimmune gastritis in cholera toxin transgenic mice. Am J Physiol Gastrointest Liver Physiol 2006, 290:G970–G979
22. Lorenz RG, Gordon JI: Use of transgenic mice to study regulation of gene expression in the parietal cell lineage of gastric units. J Biol Chem 1993, 268:26559–26570
23. Yang SH, Andl T, Grachtchouk V, Wang A, Liu J, Syu LJ, Ferris J, Wang TS, Glick AB, Millar SE, Dlugosz AA: Pathological responses to oncogenic Hedgehog signaling in skin are dependent on canonical Wnt/beta-catenin signaling. Nat Genet 2008, 40:1130–1135
24. Schumacher MA, Donnelly JM, Engevik AC, Xiao C, Yang L, Kenny S, Varro A, Hollande F, Samuelson LC, Zavros Y: Gastric Sonic Hedgehog acts as a macrophage chemoattractant during the immune response to Helicobacter pylori. Gastroenterology 2012, 142:1150–1159
25. Liu Z, Demitrack ES, Keeley TM, Eaton KA, El-Zaatari M, Merchant JL, Samuelson LC: IFNgamma contributes to the development of gastric epithelial cell metaplasia in Huntingtin interacting protein 1 related (Hip1r)-deficient mice. Lab Invest 2012, 92:1045–1057
26. Merchant JL, Saqui-Salces M, El-Zaatari M: Hedgehog signaling in gastric physiology and cancer. Prog Mol Biol Transl Sci 2010, 96:133–156
27. Martin J, Donnelly JM, Houghton J, Zavros Y: The role of sonic hedgehog reemergence during gastric cancer. Dig Dis Sci 2010, 55:1516–1524
28. Lazarevic V, Glimcher LH: T-bet in disease. Nat Immunol 2011, 12:597–606
29. Tang Q, Bluestone JA: The Foxp3+ regulatory T cell: a jack of all trades, master of regulation. Nat Immunol 2008, 9:239–244
30. Mombaerts P, Iacomini J, Johnson RS, Herrup K, Tonegawa S, Papaioannou VE: RAG-1-deficient mice have no mature B and T lymphocytes. Cell 1992, 68:869–877
31. Woo DK, Kim HS, Lee HS, Kang YH, Yang HK, Kim WH: Altered expression and mutation of beta-catenin gene in gastric carcinomas and cell lines. Int J Cancer 2001, 95:108–113
32. Oshima H, Oshima M: Mouse models of gastric tumors: wnt activation and PGE2 induction. Pathol Int 2010, 60:599–607
33. Yu H, Pardoll D, Jove R: STATs in cancer inflammation and immunity: a leading role for STAT3. Nat Rev Cancer 2009, 9:798–809
34. Li N, Grivennikov SI, Karin M: The unholy trinity: inflammation, cytokines, and STAT3 shape the cancer microenvironment. Cancer Cell 2011, 19:429–431
35. Bromberg J, Wang TC: Inflammation and cancer: IL-6 and STAT3 complete the link. Cancer Cell 2009, 15:79–80
36. Jarnicki A, Putoczki T, Ernst M: Stat3: linking inflammation to epithelial cancer—more than a "gut" feeling? Cell Div 2010, 5:14–28
37. Howlett M, Menheniott TR, Judd LM, Giraud AS: Cytokine signalling via gp130 in gastric cancer. Biochim Biophys Acta 2009, 1793:1623–1633
38. Jackson CB, Judd LM, Menheniott TR, Kronborg I, Dow C, Yeomans ND, Boussioutas A, Robb L, Giraud AS: Augmented gp130-mediated cytokine signalling accompanies human gastric cancer progression. J Pathol 2007, 213:140–151
39. Lesina M, Kurkowski MU, Ludes K, Rose-John S, Treiber M, Kloppel G, Yoshimura A, Reindl W, Sipos B, Akira S, Schmid RM, Algul H: Stat3/Socs3 activation by IL-6 transsignaling promotes progression of pancreatic intraepithelial neoplasia and development of pancreatic cancer. Cancer Cell 2011, 19:456–469
40. Grivennikov S, Karin E, Terzic J, Mucida D, Yu GY, Vallabhapurapu S, Scheller J, Rose-John S, Cheroutre H, Eckmann L, Karin M: IL-6 and Stat3 are required for survival of intestinal epithelial cells and development of colitis-associated cancer. Cancer Cell 2009, 15:103–113
41. Howlett M, Giraud AS, Lescesen H, Jackson CB, Kalantzis A, Van Driel IR, Robb L, Van der Hoek M, Ernst M, Minamoto T, Boussioutas A, Oshima H, Oshima M, Judd LM: The interleukin-6 family cytokine interleukin-11 regulates homeostatic epithelial cell turnover and promotes gastric tumor development. Gastroenterology 2009, 136:967–977
42. Ernst M, Najdovska M, Grail D, Lundgren-May T, Buchert M, Tye H, Matthews VB, Armes J, Bhathal PS, Hughes NR, Marcusson EG, Karras JG, Na S, Sedgwick JD, Hertzog PJ, Jenkins BJ: STAT3 and STAT1 mediate IL-11-dependent and inflammation-associated gastric tumorigenesis in gp130 receptor mutant mice. J Clin Invest 2008, 118:1727–1738
43. Takeda H, Nagashima R, Goto T, Shibata Y, Shinzawa H, Takahashi T: Endoscopic observation of squamous metaplasia of the stomach: a report of two cases. Endoscopy 2000, 32:651–653
44. Cho YS, Kim JS, Kim HK, Ji JS, Kim BW, Chae HS, Han SW, Choi KY, Chung IS: A squamous metaplasia in a gastric ulcer scar of the antrum. World J Gastroenterol 2008, 14:1296–1298
45. Oono Y, Fu K, Nagahisa E, Kuwata T, Ikematsu H, Yano T, Kojima T, Minashi K, Fujii S, Ochiai A, Kaneko K: Primary gastric squamous cell carcinoma in situ originating from gastric squamous metaplasia. Endoscopy 2010, 42 Suppl 2:E290–E291
46. Volpe CM, Hameer HR, Masetti P, Pell M, Shaposhnikov YD, Doerr RJ: Squamous cell carcinoma of the stomach. Am Surg 1995, 61:1076–1078
47. Sun L, Tian Z, Wang J: A direct cross-talk between interferon-gamma and sonic hedgehog signaling that leads to the proliferation of neuronal precursor cells. Brain Behav Immun 2010, 24:220–228
48. Waghray M, Zavros Y, Saqui-Salces M, El-Zaatari M, Alamelumangapuram CB, Todisco A, Eaton KA, Merchant JL: Interleukin-1beta promotes gastric atrophy through suppression of Sonic Hedgehog. Gastroenterology 2010, 138:562–572
49. Todoric J, Strobl B, Jais A, Boucheron N, Bayer M, Amann S, Lindroos J, Teperino R, Prager G, Bilban M, Ellmeier W, Krempler F, Muller M, Wagner O, Patsch W, Pospisilik JA, Esterbauer H: Cross-talk between interferon-gamma and hedgehog signaling regulates adipogenesis. Diabetes 2011, 60:1668–1676